Precoders and Equalizers for Spatially Correlated Antennas in Single-Carrier Massive MIMO Transmission

Nader Beigiparast and Ender Ayanoglu

***Abstract*—This work presents analyses of precoders and equalizers for downlink and uplink directions with different antenna structures in a single-carrier massive MIMO transmission system for a frequency selective Gaussian multiuser channel. Our work considers two different antenna formations and shows the performance of well-known precoders and equalizers in a spatially correlated channel. We show how increasing the dimension of the antenna formation can affect the system performance based on the correlation and discuss how precoding and equalizing schemes can compensate for the loss of performance due to the correlation and demonstrate the improved results.**

***Index Terms*—Uniform Linear Array, Uniform Planar Array, Precoding and Equalizing Schemes, Achievable Rate, Downlink and Uplink**

I. Introduction

The demand for high-rate wireless communications has been increasing in the past few decades [1]. Massive multiple-input multiple-output (MIMO) is one of the approaches to achieve a substantially higher rate in a wireless system [2]. The multi-user feature in a massive MIMO system offers a number of advantages compared to the point-to-point transmissions including more cost-efficient single-antenna terminals and simplified resource allocation, see [2].

As an alternative approach to OFDM, single-carrier (SC) modulation was first investigated in a massive MIMO channel in [1]. Single-carrier transmission conventionally employs adaptive equalization techniques, however, in [1], the modulation uses the precoding technique to transmit symbols over the downlink channel. In using single-carrier transmission, the main question is defining the equalization or precoding techniques in either time or frequency domain. It is noteworthy to mention that single-carrier modulation combined with frequency domain equalization or precoding is a technique similar to OFDM which is proposed to combat intersymbol interference (ISI) without the Peak-to-Average Power Ratio (PAPR) growth of OFDM, see [3]. As [1] also states that single-carrier transmission is better than OFDM for massive MIMO systems.

Previous studies have focused on the ideal case for the channel (i.e., spatially uncorrelated channel) and their approach to the system performance is based on using the optimal choice (i.e., the channel matched filter). In this work however, one can see the incorporated equalizers and precoders with the aim of maximizing the rate in the spatially correlated channel. Below, we summarize the main contribution of this work:

- We introduce a new and enhanced system model considering a well-known spatial correlation pattern.
- We prove that in the presence of correlation, the channel matched filter which was previously considered to be the optimal case does not perform well as the transmitted power grows.
- We discuss and incorporate well-known precoders in the system and further generalize the system model to be able to hold account for these techniques.
- Besides the downlink direction, we extend the work to the uplink and discuss how well-known equalizing techniques can be incorporated into the system model.
- Finally, we develop and discuss the numerical results of the channel using considered precoders and equalizers, showing the improved performance of the system over what once was thought to be optimal case.

The motivation behind this work is that with developing new techniques in the wireless communications and constant growth in the number of network users, capsulizing the massive number of antennas at the base station is inevitable. With placing the transmitters closer together, the previous assumption of transmitters being uncorrelated in space is not needed and this paper provides an analysis for this case.

This work is focused on single-carrier transmission for a massive MIMO system in a frequency selective Gaussian spatially correlated multiuser channel. In Section II, we discuss the system model in a general manner. In Section III, we discuss and elaborate on a well-known spatial correlation pattern among antenna elements that we consider in this work. Section IV is devoted to explain the models that are considered as the formation of the antenna elements. Our approach on precoding and equalizing techniques for the downlink and the uplink channels is discussed in Section V and Section VI, with presentation of the numerical results related to the performance in the system, respectively. We conclude our work in Section VII.

II. System Model

We consider a frequency-selective multiuser MIMO channel in both uplink and downlink directions, with a total of M antenna elements at the base station covering K single-antenna users. The channel between antenna element m

This work was partially supported by NSF grant 1547155.

978-1-7281-4905-9/20/$31.00 ©2020 IEEE

and user k is shown with h_{mk} and can be assumed to be independent and identically distributed (iid) with complex Gaussian distribution of zero mean and unit variance (i.e., $\mathcal{CN}(0,1)$) [1]. Also, with each use of the channel, a block of information will be transmitted that consists of T symbols (i.e., the transmission block has a length of T). Let $\mathbf{x}[t]$ and $\mathbf{u}[t]$ define the vector of transmitted and received symbols at time t, respectively. We define the vector of input and output information symbols of the channel at time t with $\mathbf{s}[t]$ and $\mathbf{y}[t]$. To be able to study the channel and examine the performance and achievable rate, we assume that the input symbols are iid with complex Gaussian distribution of zero mean and variance ρ_s (i.e., $\mathcal{CN}(0,\rho_s\mathbf{I}_K)$). Also, the additive white Gaussian noise (AWGN) in the channel is considered to be iid with zero mean, variance ρ_n, and is shown by $\mathbf{n}[t]$ at time t. Note that considering both downlink and uplink scenarios, using precoding or equalizing techniques, respectively, is commonly employed.

The channel considered in this work is assumed to have a length L, taking into account the effect of multipath on the symbols (i.e., different channel taps to model the frequency selectivity feature). One can write the relation between the vector of transmitted symbols (i.e., $\mathbf{x}[t]$) and the vector of received symbols (i.e., $\mathbf{u}[t]$) in the downlink channel for $t = 0,1,\cdots,T-1$ as

$$\mathbf{u}[t] = \sum_{l=0}^{L-1} \mathbf{H}[l]^H \mathbf{x}[t-l] + \mathbf{n}[t], \tag{1}$$

where the Hermitian of the channel matrix models the channel effect in the downlink direction. In Section V and Section VI, we will cover the precoding and equalizing techniques, respectively, and discuss how they change the input symbols to transmit over the channel. Note that in the uplink channel, the order of the channel matrix is reversed. Therefore, one can rewrite (1) for the uplink channel as

$$\mathbf{u}[t] = \sum_{l=0}^{L-1} \mathbf{H}[l] \mathbf{x}[t-l] + \mathbf{n}[t]. \tag{2}$$

The channel model consists of three major components. The first component is the correlation pattern matrix shown by $\mathbf{A}$ which is symmetric due to the symmetry property that is considered for the antenna formation. This matrix is elaborated on in Section III. The second component is the matrix of the channel between antenna elements and users (i.e., $\mathbf{H}_{\text{rand}}[l]$ for all $l = 0,1,2,\cdots,L-1$ that includes h_{mk} for all $m = 0,1,\cdots,M-1$ modeling all the antennas and $k = 0,1,\cdots,K-1$ modeling all the users) which is a random iid matrix with complex Gaussian distribution $\mathcal{CN}(0,\mathbf{I}_{M\times K})$. This matrix is fixed during each channel use, meaning it changes randomly for the next channel use (i.e., the matrix $\mathbf{H}_{\text{rand}}[l]$ is fixed for T block of symbols, it changes for the next block). The third and the last component models the channel power delay profile, it is denoted by $\mathbf{D}_{\text{fix}}[l]$ which is a diagonal matrix and its elements are $d_k[l]$ for user k in tap l. The elements of this matrix are normalized to satisfy $\sum_{l=0}^{L-1} d_k[l] = 1$ for all $k = 0,1,\cdots,K-1$ [1]. We assume that matrix $\mathbf{D}_{\text{fix}}[l]$ is fixed during the entire communication. Therefore, the channel matrix in this study is assumed to be

$$\mathbf{H}[l] = \mathbf{A}^{1/2}\mathbf{H}_{\text{rand}}[l]\mathbf{D}_{\text{fix}}[l]^{1/2}. \tag{3}$$

In order to be able to compare the results of implementing a precoder or an equalizer with other techniques in the channel, one can use the achievable rate in the system as a reference. We define the achievable rate in a MIMO channel as the following (see [1])

$$R_{\text{tot}} = \frac{1}{2}\sum_{k=0}^{K-1} \log_2\left(1 + \frac{\text{Var}\big(g_k[t]\big)}{\text{Var}\big(z_k[t]\big)}\right), \tag{4}$$

where $g_k[t]$ is the desired symbol with respect to user k at time t and $z_k[t]$ is the effective noise with respect to user k at time t. We define the effective noise and the desired symbols with respect to the users and how the precoders and equalizers affect them for the downlink and the uplink channel in Section V and Section VI, respectively. In the next section, we define the correlation pattern and how it fits into our model.

III. Spatial Correlation Pattern

In this section, a well-known correlation pattern, the exponential correlation pattern is introduced and discussed. Considering the structure of the the pattern, the correlation matrix $\mathbf{A}$ will remain symmetric [4]. It is reasonable to expect, and is evidenced in the literature, that the effect of the antenna elements on one another should be related to their distances from each other considering the dependency of the correlated channel. Let $\lambda_{i,j}$ denote the distance between antenna element m_i and antenna element m_j normalized with respect to the wavelength in the system [5]. Let Λ be the matrix of the distances which its elements are $\lambda_{i,j}$ for all i and j denoting the elements in the antenna array formation. In other words

$$[\Lambda]_{i,j} = \lambda_{i,j}. \tag{5}$$

In the exponential correlation mode, a basic correlation factor $0 < \alpha < 1$ is considered, which weighs on the effects of antennas on one another with respect to their distances, where α is a real number. One can obtain a correlation matrix based on this model in which the elements are

$$[\mathbf{A}]_{i,j} = \alpha^{\lambda_{i,j}}. \tag{6}$$

Note that taking the absolute value makes the matrix representing this model symmetric, since $|i-j| = |j-i|$. This model is commonly employed when spatial correlation is considered for MIMO or spatial diversity channels [6], [7]. The correlation coefficient increases as the separation between antennas decreases. An S-parameter-based formulation shows that when only two mono-poles are considered, the coefficient varies from 0.8 to about 0.2 when the antenna separation is about 0.05 to 0.2 times the wavelength [8]. A range of average α values from 0.4 to 0.7 for antenna separations at approximately 0.25 to 0.5 wavelength was reported in [9].

IV. Antenna Array Formation

Obtaining the distance between each antenna elements depends on the formation of antenna array. In this work, we consider two formations for the antenna elements. In the previous section, we discussed how the considered model preforms in a symmetric fashion. Considering the basic concept of symmetry in the distance between two objects and the fact that matrix **A** only depends on the correlation factor and the distance between antenna elements, it is clear that matrix **A** is symmetric. We will elaborate on the two models we have in this work for the antenna elements formation.

A. Linear Formation

In the linear formation (also known as uniform linear array), all of the antenna elements are placed on a straight line. In this formation, antenna element m_i is placed in position i and antenna element m_j is placed in position j. Therefore, one can obtain $\lambda_{i,j} = |i-j|\overline{d_n}$, where $\overline{d_n}$ is the normalized distance between adjacent antenna elements with respect to the wavelength. In this work, we assume $\overline{d_n} = 0.5$. With this in mind, one can understand all nearest neighbor distances are at exactly $\overline{d_n}$ distance from one another.

B. Rectangular Formation

We consider the rectangular 2D-formation for the antenna array (also known as uniform planar array) as the second formation model. The total number of antennas can be written as $M = M_{\text{row}} \times M_{\text{col}}$ where M_{row} and M_{col} indicate the number of antennas at each row and column, respectively. Considering the rectangular structure, one can understand that the distance matrix for each row of the formation has the same structure as that for the 1D array. Hence, one can say the distance matrix has the same linear property (increasing linearly as the indices increase) for the antenna elements in the same row or column. For calculating the distances of the antenna elements in different rows, one only needs to add offsets indicating the difference between the row indices and the column indices to obtain the distance between the certain antenna elements in the formation. We define r_m as the position of antenna element m in the rows of the structure. Therefore, one can understand that r_m is an integer ranging from 0 to $M_{\text{row}} - 1$. In other words, r_m can be stated as

$$r_m = \lfloor \frac{m}{M_{\text{row}}} \rfloor, \tag{7}$$

where it means r_m is the closest integer less than or equal to the result of the fraction (i.e., $r_m = \text{floor}\big(m/M_{\text{row}}$ indicating the row that includes antenna element m). In a similar manner, one can obtain the positioning of antenna element m in the columns of the antenna structure as

$$c_m = m - r_m M_{\text{row}}, \tag{8}$$

where c_m is also an integer ranging from 0 to $M_{\text{col}} - 1$.

Considering the different positioning for antennas elements in the two dimensional structure, one can obtain a general formula to calculate the distance between antenna element i and antenna element j as the following

$$[\Lambda]_{i,j} = \overline{d_n}\sqrt{\zeta^2 + |c_i - c_j|^2}, \tag{9}$$

where $\zeta = |r_i - r_j|$ works as the offset. Note that one can obtain c_i and c_j using (8), and r_i and r_j using (7).

In the next section, the precoding techniques will be introduced and the result of an evaluation of the performance of the system will be provided in a spatially correlated downlink channel.

V. Downlink Channel

For the downlink direction, we do not consider any equalizers in the system, carrying all the necessary computation to the base station side. Therefore, the vector of the received symbols and the vector of the output symbols are the same (i.e., $\mathbf{y}[t] = \mathbf{u}[t]$) in this model. Let $\mathbf{P}[l]$ be the precoding matrix in tap l of the channel. Note that since we define the precoding process in the frequency domain, one can transform the precoding matrix to and from the frequency domain using Ω-point Fourier or inverse Fourier transform [4]. Let $\mathbf{P}[\omega]$ define the precoding matrix in the frequency domain where $\omega = 0, 1, \cdots, \Omega-1$. In order to normalize the precoding matrix, we will consider a normalization factor so that

$$\mathbb{E}\big\{|\mathbf{P}[\omega]|^2\big\} = 1. \tag{10}$$

Having the precoding matrix, one can obtain the vector of transmitted symbols from the vector of input symbols as (for more details on how precoder affects the input symbols, see [1])

$$\mathbf{x}[t] = \sum_{l=0}^{L-1} \mathbf{P}[l]\mathbf{s}[t+l]. \tag{11}$$

By replacing (11) in (1) and knowing that in the downlink channel, $\mathbf{u}[t] = \mathbf{y}[t]$, one can obtain the vector of output symbols of the system as

$$\mathbf{y}[t] = \sum_{l=0}^{L-1}\sum_{l'=0}^{L-1} \mathbf{H}[l]^H \mathbf{P}[l']\mathbf{s}[t-l+l'] + \mathbf{n}[t]. \tag{12}$$

In order to be able to examine the performance of the channel in the downlink, we need to define the desired symbols with respect to each individual user.

In the downlink channel, the desired symbols can be expressed as the expected value over the terms which user k is supposed to receive (not considering the noise). Hence, one can write the vector of desired symbols as

$$\mathbf{g}[t] = \sum_{l=0}^{L-1} \mathbb{E}\big\{\mathbf{H}[l]^H \mathbf{P}[l]\big\}\mathbf{s}[t], \tag{13}$$

where **g**[t] represents the vector of desired symbols for all the users. The effective noise can be obtained by subtracting the vector of desired symbols from the vector of output symbols (i.e., $\mathbf{z}[t] = \mathbf{y}[t] - \mathbf{g}[t]$). In each of the following subsections, different precoding techniques have been introduced and elaborated on.

A. Channel Matched Filter Precoder

As it can be understood from its name, the channel matched filter (CMF) precoder matches the channel response to obtain the result and it can be defined as

$$\mathbf{P}[l] = \varphi_c \mathbf{H}[l], \tag{14}$$

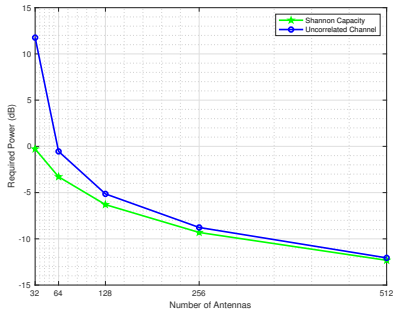

Fig. 1. Performance of the CMF Precoder compared to Shannon's capacity. The achievable rate is considered to be $R_{tot} = 10$ bpcu in a system supporting $K = 10$ users.

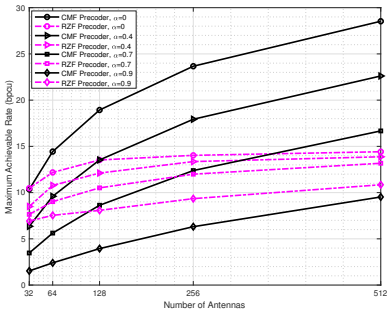

Fig. 2. System performance of CMF and RZF precoders with the linear antenna formation in a downlink channel with different correlation factors supporting $K = 10$ users in a channel with length $L = 4$, transmitting $T = 100$ symbols in each channel usage.

where φ_c is a normalization factor in order to satisfy (10). By placing (14) in (12) and (13), one can simplify the equations for the vector of output symbols and the vector of desired symbols. Therefore, it is possible to obtain a closed form expression for the equations for the vector of desired symbols and the vector of effective noise in the system. As it is stated in [1], [4], the power of the desired symbol with respect to user k can be expressed as the following

$$\mathrm{Var}\{g_k[t]\} = \frac{M}{K}\rho_s, \tag{15}$$

and the power of the effective noise with respect to user k can be written as

$$\mathrm{Var}\{z_k[t]\} = \frac{\mathrm{tr}(\mathbf{A}^2)}{M}\rho_s + 1, \tag{16}$$

where $\mathrm{tr}(\mathbf{A}^2)$ shows the trace of the correlation matrix to the power of two. Using (15) and (16) in (4), one can determine the performance of the system equipped with CMF precoder. The achievable rate of the system can be stated as (for more details on how to derive the following, see [4])

$$R_{\mathrm{tot}}^{\mathrm{CMF}} = \frac{1}{2}\sum_{k=0}^{K-1}\log_2\left(1 + \frac{M^2\rho_s}{K\mathrm{tr}(\mathbf{A}^2)\rho_s + MK}\right), \tag{17}$$

Fig. 1 shows the performance of the system equipped with CMF precoder in an uncorrelated downlink channel and compares it with the Shannon's capacity [1]. Note that since the uncorrelated channel is considered in this figure, the formation of the antennas does not matter. In the considered system, the required power is measured with respect to the number of antennas at the base station in order to obtain the total rate of $R_{tot} = 10$ bit per channel use (bpcu). The gap between two curves starts to fade as the number of antennas increases [1]. Note that the channel has length $L = 4$ and each transmission block has length $T = 100$ symbols.

B. Regularized Zero Forcing Precoder

The Regularized Zero Forcing (RZF) precoder aims to maximize the power of the desired signal compared to the power of the noise and interference at the receiver using β_p known as the RZF power parameter which depends on the users path losses and input signal to noise ratio (SNR) and improves the performance of the precoder. RZF precoder matrix can be written as

$$\mathbf{P}[l] = \varphi_r\mathbf{H}[l]\left(\mathbf{H}[l]^H\mathbf{H}[l] + \beta_p\mathbf{I}_K\right)^{-1}, \tag{18}$$

where φ_r is the normalization factor specified for RZF precoder and $\mathbf{I}_K$ is the identity matrix with the size of $K\times K$. One can obtain the achievable rate in the system using RZF precoder as the following

$$R_{\mathrm{tot}}^{\mathrm{RZF}} = \frac{1}{2}\sum_{k=0}^{K-1}\log_2\left(1 + \frac{\mathrm{Var}(g_k[t])}{\mathrm{Var}(z_k[t])}\right), \tag{19}$$

where $g_k[t]$ is (13) for k-th user and $z_k[t] = y_k[t] - g_k[t]$ as stated in [4].

A comparison between the performance of CMF precoder and RZF precoder is done and shown in Fig. 2 and Fig. 3 for the downlink channel with the linear antenna formation and the rectangular antenna formation, respectively. The length of the channel in the frequency domain is considered to be $\Omega = 20$ (the number of points to compute the Fourier transform). As it can be seen, with the linear formation in Fig. 2, RZF precoder will outperform CMF precoder in terms of the maximum achievable rate possible in the system in a highly correlated downlink channel (i.e., $\alpha = 0.9$). With the rectangular formation on the other hand, there can be seen a noticeable gap between the two precoders in smaller values of correlation pattern factor (i.e., $\alpha = 0.7$) compared to the same channel with linear formation. The common feature in both figures is the fact that with increasing the correlation factor, the loss of achievable rate is significantly higher for the system equipped with CMF precoder than that equipped with RZF precoder. One can easily spot that the curves of RZF precoder are much closer to one another in comparison with those of CMF precoder.

Also, note that for a smaller number of antennas and smaller values of correlation parameter, the maximum achievable rate for RZF precoder is slightly higher, however, by increasing the number of antennas, RZF precoder loses its advantage to the relatively higher slop of gaining achievable rate of the CMF precoder. CMF precoder slows down as the correlation parameter increases, leading to the full superiority of RZF precoder.

VI. Uplink Channel

Using the same argument for the downlink channel, we only consider equalizing techniques in the uplink and no precoding techniques in order to relocate any computations

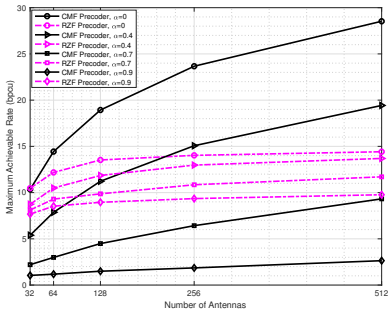

Fig. 3. System performance the precoders with the rectangular antenna formation in a correlated downlink channel of length $L = 4$ supporting $K = 10$, with $T = 100$ symbols in each channel usage.

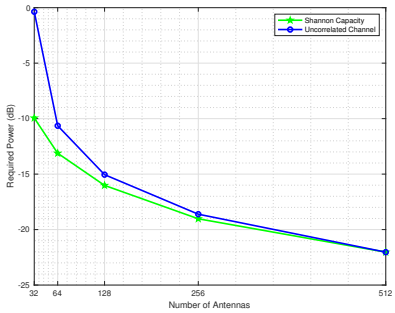

Fig. 4. A comparison between performance of CMF equalizer and the system's capacity to achieve $R_{tot} = 10$ bpcu supporting $K = 10$ users, sending $T = 100$ symbols per channel use with $T_c = 20$ cyclic prefix.

needed to the base station side. However, in order to maintain the circular convolution property in the uplink equations, we use the cyclic prefix technique. In this work, we use the conventional cyclic prefix technique, where the last T_C samples of a T-sample transmission block are added to the beginning of the block. Note that in this work, the cyclic prefix is designed in the way that the length of the added symbols are larger than the length of the channel (i.e., $T_c > L$). Using $\mathbf{Q}[l]$ to define the equalizing matrix in the channel for tap l and $\mathbf{Q}[\omega]$ to show its counterpart in the frequency domain at frequency $\omega = 0, 1, \cdots, \Omega-1$, one can define the relationship between the vector of output symbols $\mathbf{y}[t]$ and the vector of received signals $\mathbf{u}[t]$ in the frequency domain as the following

$$\mathbf{y}[\omega] = \mathbf{Q}[\omega]\mathbf{u}[\omega], \tag{20}$$

where $\mathbf{u}[\omega]$ and $\mathbf{y}[\omega]$ are the frequency domain representation of $\mathbf{u}[t]$ and $\mathbf{y}[t]$, respectively. Note that same as the precoding matrices, the equalizing matrix is normalized so that

$$\mathbb{E}\{|\mathbf{Q}[\omega]|^2\} = 1. \tag{21}$$

By transforming (20) to the time domain, one can obtain the relationship between the vector of received symbols and the vector of output symbols in the time domain in the way we define it here as

$$\mathbf{y}[t] = \sum_{l=1}^{L} \mathbf{Q}[l]\mathbf{u}[t-l], \tag{22}$$

where $t-l$ in $\mathbf{u}[t-l]$ is calculated using $\bmod T$. By replacing (22) in (2), one can simplify the equation for the vector of output symbols of the system as

$$\mathbf{y}[t] = \sum_{l=0}^{L-1}\sum_{l'=0}^{L-1} \mathbf{Q}[l']\mathbf{H}[l]\mathbf{s}[t-l-l'] + \sum_{l=1}^{L} \mathbf{Q}[l]\mathbf{n}[t-l]. \tag{23}$$

We define the vector of desired symbols in the uplink channel as

$$\mathbf{g}[t] = \sum_{l=1}^{L} \mathbb{E}\{\mathbf{Q}[-l]\mathbf{H}[l]\}\mathbf{s}[t]. \tag{24}$$

In the same way that we derived th effective noise term in the downlink channel, one can obtain the effective noise of the uplink channel (i.e., $\mathbf{z}[t] = \mathbf{y}[t] - \mathbf{g}[t]$). Using the desired symbols and the effective noise in the system for k-th user, one can obtain the achievable rate using (19).

A. Channel Matched Filter Equalizer

CMF equalizer can be defined in the same way as the one in the downlink channel

$$\mathbf{Q}[l] = \varphi_c \mathbf{H}[l]^H, \tag{25}$$

where φ_c is a factor to satisfy (21). Using (25) in (23) and (24), the equations for the vector of output symbols and the vector of desired symbols is feasible and hence, it enables us to examine the performance of the system under the influence of the spatial correlation pattern.

One can see the performance of CMF equalizer in comparison with the Shannon's capacity in Fig. 4, where the channel length in the time domain is set to $L = 4$ and in the frequency domain to $\Omega = 20$. The gap starts to fade away as the number of antennas increase, meaning the performance of CMF equalizer goes to near-optimally in low-SNR regions for larger number of antennas. The general behavior of CMF equalizer is similar to CMF precoder as it can be seen in Fig. 1.

B. Minimum Mean Square Error Equalizer

In a very similar manner to RZF precoder in the downlink, the minimum mean square error (MMSE) equalizer has the upper hand of using power parameter to enhance the system behavior. MMSE equalizer matrix can be written as

$$\mathbf{P}[l] = \varphi_m \big(\mathbf{H}[l]\mathbf{H}[l]^H + \beta_q \mathbf{I}_K\big)^{-1}\mathbf{H}[l], \tag{26}$$

where β_q is the power parameter for MMSE equalizer. The comparison between the performance of the system in the spatially correlated uplink channel using CMF and MMSE equalizers is shown in Fig. 5 and Fig. 6 for the linear formation and the rectangular formation, respectively. The length of the transmission block is considered to be $T = 100$ with $T_c = 20$ cyclic prefix symbols added to the transmission block, and the length of the channel is $L = 4$ in the time domain and $\Omega = 20$ in the frequency domain. As it can be seen, MMSE equalizer outperforms CMF equalizer even for the lower values of the correlation parameter. Unlike the downlink scenario, where CMF precoder starts with the higher slope, in the uplink channel, both equalizers perform in about the same slope, meaning that CMF equalizer do not have the upper hand for the cases with a fewer number of antennas. As the correlation factor increases, the gap between the curves for CMF equalizer also increases (relatively to

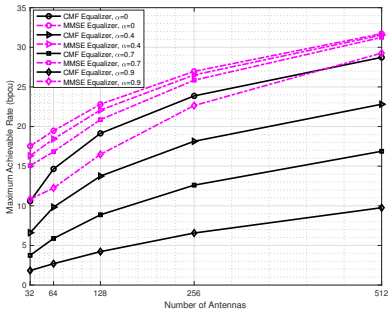

Fig. 5. Maximum achievable rate of CMF and MMSE equalizer in the correlated uplink channel with linear antenna formation supporting $K = 10$ users.

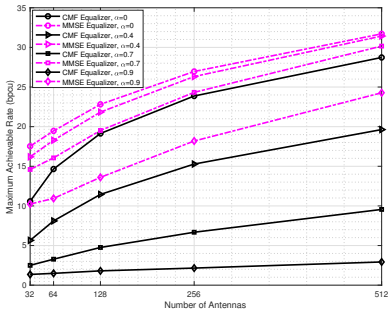

Fig. 6. Performance of CMF equalizer and MMSE equalizer in a spatially correlated uplink channel with the rectangular antenna formation for $K = 10$ users.

those of MMSE equalizer). One can note that the maximum achievable rate in the system with MMSE equalizer is significantly higher than that with CMF equalizer and the gap between the performance of the two equalizers increases with the growth of the correlation factor.

VII. Conclusion

Based on the calculations and the results in Section VI and Section V, one can see that the performance of the system is enhanced using the suggested precoder or equalizer when the channel is considered to have spatial correlated elements at the base station side. RZF precoder in the downlink channel can slightly enhance the performance in terms of the maximum achievable rate comparing to CMF precoder when the correlation increases. By looking at Fig. 2, it can be seen that the slope of the curves of CMF precoder starts off higher, meaning CMF precoder is more capable of achieving higher rates in a low-correlated downlink channel. However, increasing the correlation factor causes a significant decrease in the performance, to the point that in a downlink channel with correlation factor $\alpha = 0.9$ and the total number of transmitters $M = 512$, the total maximum of achievable rate is less than 10 bpcu for $K = 10$ users. For the same downlink channel, RZF precoder maximum achievable rate curve stays above that of CMF precoder for all the considered values for the total transmitters. The decrease in the performance of CMF precoder is more dramatic when it comes to the rectangular antenna array formation, seen in Fig. 3. One can see that the curve for RZF precoder maximum achievable rate stays above that of CMF precoder for smaller value of the correlation parameter, indicating the better performance of the suggested precoder for the two-dimensional antenna formation as well.

The same behavior can be seen for the uplink, the superiority of the suggested equalizer over CMF equalizer even for the lower values of the correlation parameter. Looking at Fig. 5, the performance of MMSE equalizer is not as sensitive to the correlation factor as CMF equalizer is, and the latter outperforms the former in terms of the maximum achievable rate possible for all the values of the correlation factor considered. One can easily see that the curves for MMSE equalizer are above those of CMF equalizer for all the considered values of correlation parameter and the total number of antennas at the base station. The decrease in the performance of the CMF equalizer worsens as the correlation factor grows. MMSE equalizer on the other hand, shows a significant achievable rate, even for a highly correlated channel. The gap between the two equalizers increases as one moves from the linear formation to the rectangular in Fig. 6. MMSE equalizer outperforms CMF equalizer in the tow-dimensional formation as well.

By looking at the figures in the two previous sections, one can state that the suggested precoding and equalizing schemes have better potentials on achieving more data rate in a system with multiple transmitters and receivers under the influence of spatial correlation. Note that this study considers a range of correlation factors and the total number of antennas at the base station, where it is conceivable that the behavior stays the same for the larger number of antennas or different range of correlation parameter.

References

[1] A. Pitarokoilis, S. K. Mohammed, and E. G. Larsson, "On the optimality of single-carrier transmission in large-scale antenna systems," *IEEE Wireless Commun. Lett.*, vol. 1, pp. 276–279, Aug 2012.

[2] E. G. Larsson, O. Edfors, F. Tufvesson, and T. L. Marzetta, "Massive MIMO for next generation wireless systems," *IEEE Commun. Mag.*, vol. 52, pp. 186–195, Feb 2014.

[3] D. Falconer, S. L. Ariyavisitakul, A. Benyamin-Seeyar, and B. Eidson, "Frequency domain equalization for single-carrier broadband wireless systems," *IEEE Commun. Mag.*, vol. 40, pp. 58–66, Apr 2002.

[4] N. Beigiparast, G. M. Guvensen, and E. Ayanoglu, "The effect of antenna correlation in single-carrier massive MIMO transmission," in *IEEE 87th Vehicular Technology Conference – Spring*, Jun. 2018, pp. 1–7.

[5] A. Abdi and M. Kaveh, "A space-time correlation model for multielement antenna systems in mobile fading channels," *IEEE J. Sel. Areas Commun.*, vol. 20, pp. 550–560, Apr 2002.

[6] V. A. Aalo, "Performance of maximal-ratio diversity systems in a correlated Nakagami-fading environment," *IEEE Trans. Commun.*, vol. 43, pp. 2360–2369, Aug 1995.

[7] E. Bjornson, E. Jorswieck, and B. Ottersten, "Impact of spatial correlation and precoding design in OSTBC MIMO systems," *IEEE Trans. Inf. Theory*, vol. 9, pp. 3578–3589, Nov 2011.

[8] X. Wang, H. D. Nguyen, and H. T. Hui, "Correlation coefficient expression by S-parameters for two omni-directional MIMO antennas," in *IEEE Int. Symp. Antennas Propag. (APSURSI), Spokane, WA, 2011*, Jul 2011, pp. 301–304.

[9] M. K. Samimi, S. Sun, and T. S. Rappaport, "MIMO channel modeling and capacity analysis for 5G millimeter-wave wireless systems," in *10th European Conference on Antennas and Propagation (EuCAP)*, Apr 2016.